Next Materials 2 (2024) 100121

Contents lists available at ScienceDirect

Next Materials

journal homepage: www.sciencedirect.com/journal/next-materials

Research article

Impact of short-time annealing on AISI 8670 tool steel saw during industrial brazing process

Ludovic Jego [a], Majid Heidari [b], Muftah Zorgani [a,*], Tom Levasseur [b], Mohammad Jahazi [a]

[a] École de technologie supérieure, Département de Génie Mécanique, Montreal, QC H3C 1K3, Canada
[b] DK-Spec, 1060 Chem. Olivier, Lévis, QC G7A 2M8, Canada

ARTICLE INFO

Keywords:
Metallurgical engineering
Saw
Tool steel
Brazing
Microscopic characterisation and microanalysis
Residual stress
Manufacturing defect
Short-time annealing

ABSTRACT

This study is focused on determining the impact of short-time annealing during industrial brazing process. Short-time annealing is commonly used to alleviate residual stresses resulting from the brazing process and represent in this study 30% of the process time. Samples were selected using two designs of experiments with three main parameters which are temperature of brazing, temperature of short-time annealing and time of first cooling for the first, and temperature of brazing for the second. Shear resistance tests allowed to refine the selection of samples for further investigation. EDS views, hardness measurements and residual stress measurements were conducted. From the obtained results, although slight differences were observed in the microstructure, hardness, and residual stresses of the samples, no clear pattern of impacts could be attributed to short-time annealing. In conclusion, this study did not find substantial evidence of short-time annealing having a significant impact on the microstructure, hardness, or residual stresses in the context of industrial brazing for wood cutting tools. Further research could explore other annealing parameters or alternative heat treatment methods to achieve the desired material properties.

1. Introduction

The wood industry is one of the most prolific in Canada, which creates a lot of jobs. Wood cutting is one such job category, and involves the use of tools mostly made of tool steel [1]. However, tools used in this industry may face hard particles such as rocks, lead which can impact the quality of the wood. To combat that, specific cutting tools, such as those made of tungsten carbide, are used. These tools are characterized by a very high hardness and relatively good toughness and resistance to wear and erosion [2–6]. Because of cost constraints, tools cannot simply be made entirely from tungsten. To overcome this, processes such as brazing are used to join tungsten to other materials to maximize the mechanical properties of the tools [7,8].

The brazing process is highly valued in industry because of its simplicity of application and relatively low cost [9]. It is a joining technique that proceeds by adding a certain material, and that consists of three main steps: i) assembly of the joint zone, whose temperature is then raised to reach the melting temperature of the filler material, but not that of the rest of the assembly; ii) production of good wetting conditions for the filler material between the tungsten carbide and the steel substrate to create a seal between them; iii) cooling of assembly under specific conditions once the seal is in place. In this process, though, the joint may break or become separated and products may sustain damage.

Although the brazing technique is well-known for its simplicity, the brazed joint is, however, heterogeneous in nature, as it involves different phases, with each having different physical and chemical properties. Moreover, the presence of porosity, segregation of elements, and residual stresses during cooling could all contribute to the fragilization of the joint and lead to failures located in the joint but also in other areas of the brazed product [10,11]. Therefore, in order to achieve optimum joint properties, it is of critical importance to better understand the interactions between process parameters and joint quality in terms of microstructural homogeneity as well as mechanical properties.

The quality of brazed joints depends on various process parameters, with brazing temperature and time being particularly crucial, as reported by many authors [12–16]. A better understanding of the influence of these parameters is essential in industry as it could result in significant cost reductions but also a reduction of the failures during production. These failures can be due to residual stress concentration

* Corresponding author.
E-mail address: muftah.zorgani@etsmtl.ca (M. Zorgani).

https://doi.org/10.1016/j.nxmate.2024.100121
Received 20 November 2023; Received in revised form 20 December 2023; Accepted 10 January 2024
Available online 8 February 2024
2949-8228/© 2024 The Author(s). Published by Elsevier Ltd. This is an open access article under the CC BY license (http://creativecommons.org/licenses/by/4.0/).

Table 1
Chemical composition of different materials of the study (wt%).

AISI 8670	C	Ni	Mo	Mn	Cr	Si	P	S
Steel	0.75%	1.00%	0.10%	0.60%	0.50%	0.30%	0.025%	0.025%
TMK22	**WC**	**Co**						
Tungsten carbide tip	94.0%	6.0%						
Brazetec 4900 A	**Ag**	**Ni**	**Wn**	**Mn**	**Cu**			
Filler metal	49.0%	0.5%	20.5%	2.5%	27.5%			

induced by differences between the coefficient of thermal expansion of the brazed materials [17]. Furthermore, production parameters have a direct impact on the strength of the joint, as highlighted in [18]. One of the key factors used to assess the quality of a brazed joint is its shear strength. Extensive research efforts, exemplified by references [19–21], have been dedicated to studying the impact of brazing process parameters on the shear strength of the joint. It must be noted that both temperature of brazing and holding time of this temperature during brazing process influence the microstructure of the brazed joint [22,23]. Specifically, as reported by Gambaro et al., [24], brazing temperature and time impact the growth of intermetallic compounds, and could lead to a reduction in the mechanical properties of the joint, including bonding strength, [19,24,25], or even failures in the joints with appearance of micro-cracks, as shown by Wang et al., [19].

The filler metal plays a crucial role in achieving a successful brazed joint. These include, but not limited to: its fluidity, stability during operation, wettability, volatility rate, ability to create bonds with the base materials, erosion and surface condition. In addition, the wetting includes various factors such as the contact angle with the surface, the energy of the surface, etc. Among the challenges, the much lower wettability of ceramic materials (e.g., tungsten carbide) and the difference in thermal expansion coefficient between the ceramic and the metal substrate need to be studied and optimized for the specific alloys and joint design in the present project. Additional elements in the filler material [26–29] could also improve the wettability by allowing a better spreading of the filler material [27].

In industrial brazing, annealing is the last step in the process. Indeed, brazing induces stresses during production and annealing is a solution for this issue [30,31]. Because of the short time of the process, this part of the thermal cycle is called short-time annealing [32–34]. The selection of the short-time annealing temperature, has a significant impact on the residual stresses, microstructure and hardness [30,31,34–37]. To this extent, the annealing step is proceeded in the area most affected by the heat during the process and presenting issues, i.e., the end of the heat affected zone on the shoulder of the saw.

Annealing also has some impacts on other material properties linked to residual stress, such as the microstructure and the hardness [38,39]. Although it is common practice in industry to proceed with short-time annealing after brazing, only limited information is available on the impact of the annealing process on brazed products for wood cutting tools.

The aim of the present article is to study the impact of the short-time annealing process on brazed cutting tools for the wood industry as a way to reduce failures induced by the process. Accordingly, samples were selected via a Design of Experiments (DoE). The annealing portion of the thermal cycle represents about 30% of the total process time. This study compares two different thermal cycles of the brazing process in a bid to provide an understanding of the impact of a fast anneal on the mechanical properties of the saw and of the brazed jaw during the thermal cycle. A mechanical analysis was performed on selected samples representing different thermal cycles and different shear resistance values to adjudicate over the interest of short-time annealing during brazing.

2. Experimental procedure

2.1. Materials used

The test specimen for this study consists of three components: a steel substrate, filler material and tungsten carbide. AISI 8670 tool steel, a low alloy steel mostly used in the wood industry for the production of circular saw bodies, was selected [40]. Its chemical composition is presented in Table 1. JMATPro software was used to run an analysis over AISI 8670. The software allows a better understanding of the material by modeling its properties and behavior [41]. CCT and TTT analyses were thus run, and will be discussed later in this paper. The saw used for this study, made with this steel, are 3.05 mm thick, and 304.80 mm in diameter.

Tungsten carbide tips used in this work is commercially available from Techmet, and is referenced as TMK22. Its chemical composition is presented in Table 1. Its tips are 3.3 mm large, 12.8 mm long, and 5.94 mm thick.

Filler material is used for bonding. It is furnished with a flux for properly preparing the surface to allow better bonding. It is a Silver-Copper base material and is commercially available as Brazetec 4900 A. The material is 3 mm large, 0.3 mm thick, and 12.8 mm long. The flux used during this process, as recommended by the seller, is Brazetec h285 Paste.

All the chemical compositions are detailed in Table 1:

The production was realized entirely on an automatic brazing machine, the Ferling Automation GLL. The parameters used for the production were selected via a Design of Experiments (DoE) realized in collaboration with the industrial partner, and are specified in the next section.

2.2. Selected samples

Samples were produced with different production parameters on the Ferling Automation GLL. This machine allowed an automatic precision brazing programmable process for the dosing of flux, follow of the temperature, positioning of the tips and versatility allowing to work with different geometry of circular saws, tips or filler materials [42]. That is why the selection of the samples for this study was done with this parameter as first criteria of selection to compare different products produced across different thermal cycles. Because of the high number of parameters involved in the process, a DoEs was selected as a route in order to reduce number of samples produced.

Two distinct DoEs were realized, one for each thermal cycle. The parameters considered were the brazing temperature and the annealing temperature and first cooling time[18,22,38,39]. Other parameters, such as the brazing time and the annealing time, were set for this work. A surface response center composite with 3 parameters was selected for the thermal cycle with short-time annealing and D-Optimal plan with one factor was run for the thermal cycle without short-time annealing. D-Optimal in the only DoE method that allows working with just one factor. The surface response center composite was selected over the Box-Behnken design because it provides better prediction results [43,44]. Minitab and Design Expert were used to create the DoEs with factors chosen to minimize the number of tests/specimens, with 33 samples produced in total, as compared to more than 100 without this method.

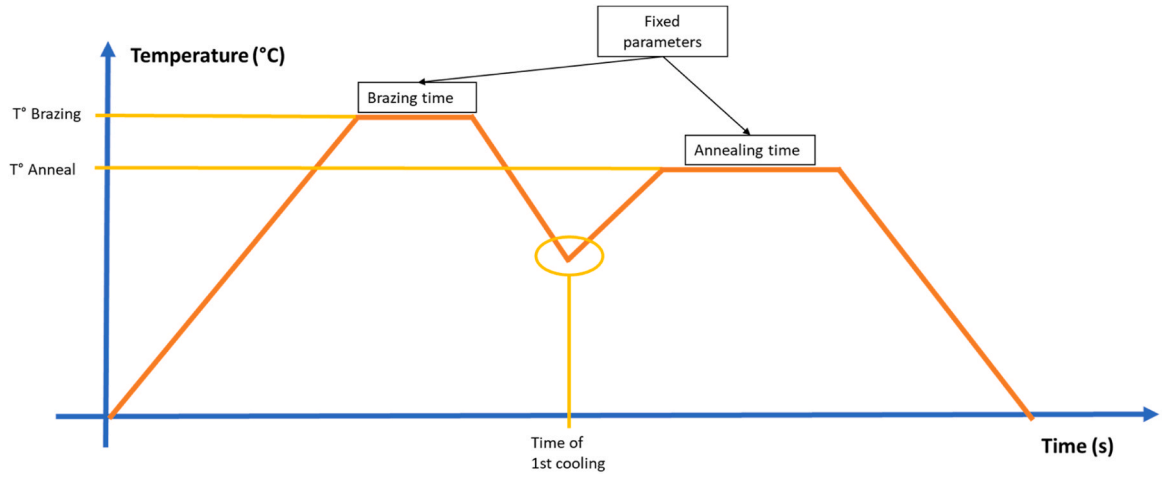

Fig. 1. Thermal cycle of industrial brazing process at DK-Spec.

The production thermal cycle can be illustrated as in Fig. 1:

Fig. 1 highlights the three main parameters used as inputs for the DOEs, namely brazing temperature, annealing temperature and the time of 1st cooling which could be changed during production process. Among these parameters, brazing and annealing times were fixed according to industrial practice. Inputs for the DOEs were evolving in the intervals defined by industrial practices.

Inputs were changed for the DoEs according to ranges of work used during normal production time and according to documentation from the supplier of filler metal and flux [45,46]. The brazing temperature was thus changed from 680 and 720 °C, the annealing temperature from 450 to 600 °C, and finally, the time of 1st cooling, from 1.5 to 2.5 s

Samples were selected over their results at shear tests [47]. The GLFPE Brazing bond strength measuring unit was used to run the tests. Samples were prepared to measure the layer thickness and shear resistance of intermetallic compounds (IMCs). The shear tests are destructive, but were run in a controlled area with the same operator. Firstly, IMC layer thickness and shear resistance results were analyzed, but because of the distribution of those results. Selection of the samples will use as primary criteria results over shear resistance tests. Moreover, to reduce the number of samples to be analyzed in greater detail, it was decided to consider only the best and worst samples in terms of shear strength test results. The surface and thickness will be further investigated during this study, which means samples will be tested in both directions. As such, for each thermal cycle, 2 samples represent surface tests, and 2 samples represent thickness tests.

2.3. Analysis

All the tests performed involved the use of different analysis techniques. For the microstructure analysis, two different instruments were used, namely, the SEM Hitachi TM-3000 with an EDS module and the Lext 4100 confocal microscope.

JMATPro software was used to obtain CCT and TTT results for the AISI 8670 used in this study. Fiji software was used for the analysis of the microstructure views. A thickness measurement module was used to measure the IMCs' layer thickness. Residual stress measurements were performed using Pulstec x360. This machine allows to measure residual stress on the surface of samples via the x-ray diffraction method. Finally, hardness measurements were realized on a Struers Duramin 40 according to ASTM A370–22 and E92–17. The Vickers method was used, with a holding time of 10 s, with two different loads, HV_{10} and $HV_{0.2}$, depending on the direction of measurement. Hardness tests and residual stress measurements were performed at ambient temperature. For each sample, location and test, at least three tests were done, and the average hardness and residual stress values were used.

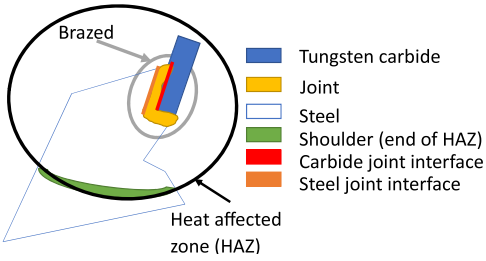

Fig. 2. Schema of surface view of saw's teeth with zones of interest.

2.4. Preparation

All the samples were analyzed on different machines and were prepared with polishing paper and solution up to 1 μm. For the microstructure, etching with Nital 3% was done for 10 s before an analysis was performed on a microscope.

As Fig. 2 shows, a single sample presents different zone of interest. This figure represents a view of a saw's teeth. It allows to highlight the zones of interest, namely, the joint area, the heat affected zone (HAZ), and more especially, the shoulder, which is at the end of the HAZ.

As is shown in Fig. 3, samples were cut in thickness direction, after which they were mounted. In this study, there are different zones that deserve in-depth research. They are located all over the samples and especially in the HAZ. According to the manufacturer of the saws, particular attention was paid to the end of the HAZ. Indeed, fracture or bending occur in this zone, called the shoulder zone. In this way, the process implies an annealing process applied on the shoulder area; therefore, residual stress measurements were made only in the shoulder zone.

3. Results and discussion

3.1. Shear resistance tests for samples selection

For both DoEs, measurements of the intermetallic compounds layer were realized. The SEM TM3000 was used to capture images, which were then processed using Fiji software to calculate the thickness of the layer. The SEM examination allowed to observe the interface between the different parts of the system. In a preliminary study, it was observed that when the samples fractured, a crack propagated from the interface between the joint and the carbide. A continuous layer of intermetallic compounds is observed along the entire interface. Fig. 4 illustrates the resulting analysis from the image to the software.

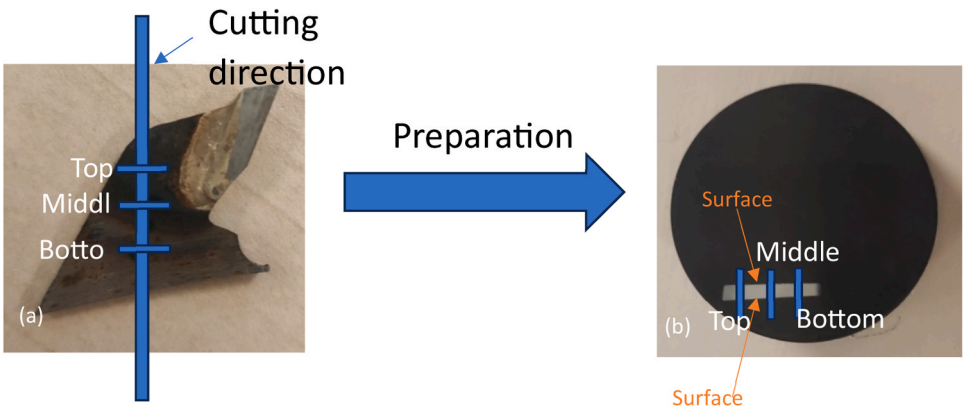

Fig. 3. Preparation steps to obtain thickness samples to analyze: (a) produced sample, (b) sample enrobed for analysis and positioned in thickness direction.

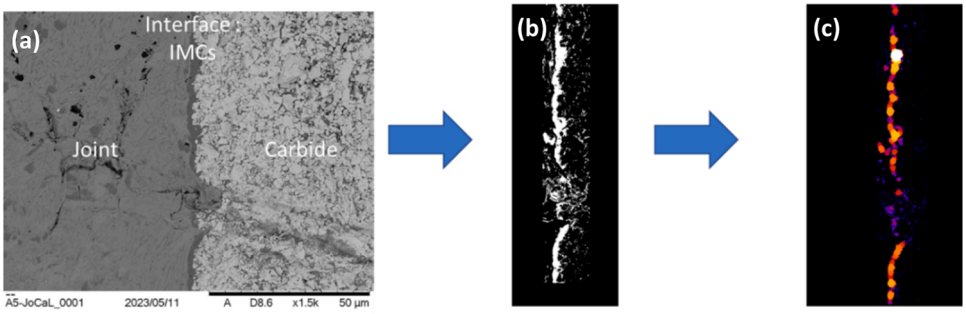

Fig. 4. TM3000 view analyzed with Fiji software for IMCs layer measurement: (a) TM3000 view; (b) Highlight of IMCs with Fiji; (c) Thickness measurement with Fiji.

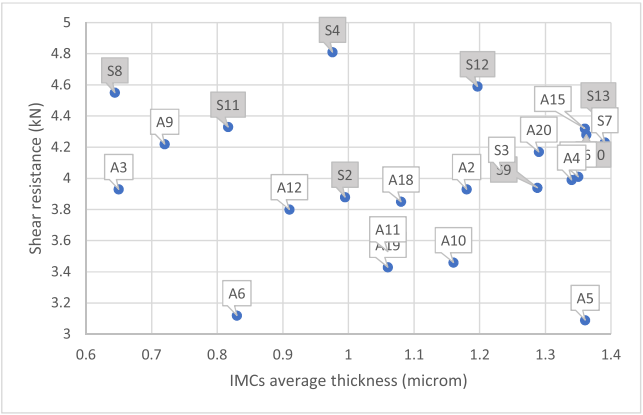

Fig. 5. Shear strength as a function of average IMCs layer thickness for brazed saw samples.

The measurement results were compared with results from shear strength tests to identify any relation between both properties. Both results are detailed in Fig. 5.

This analysis indicates that there is no significant relation between the shear strength and thickness of the IMCs layer. The literature shows that there is an optimum thickness at which layers maximize their shear resistance [48,49]. Moreover, it also indicates that an optimum shear strength value is obtainable with the specific brazing temperature [50]. The temperature will thus impact both the shear resistance and the thickness of the IMCs layer [51]. However, this is not visible in the present work. All the samples tested and both thermal cycles did not seem to identify any impact of a thermal cycle with short annealing on the shear resistance or IMCs layer thickness. Further analyses were conducted on a reduced number of samples.

The samples selected from the first thermal cycle with annealing, along with their fabrication parameters, are listed in Table 2.

The selected sample from this second thermal cycle with parameter of fabrication and results over shear tests are listed in another table, Table 3.

Four samples were selected for each cycle. Results for shear resistance tests were not analyzed because they only served as a criterion of selection of the samples for this study [19–21,47].

Microstructure, hardness and residual stress analysis were conducted to quantify the impact of short-time annealing step during an industrial brazing process on circular wood saws.

3.2. Shoulder microstructure

An analysis using JMATPro software in Fig. 6, which illustrates the TTT diagram, shows that depending on the time of the process and the cooling rate, microstructural changes can occur, with transitions between pearlite, bainite and ferrite.

That simulation is an initial analysis to study the microstructure of the base material, as received AISI 8670. Microscopic examinations were realized on surface and through the thickness. SEM observations, realized on TM3000, revealed the presence of large size particles as well as laths that are probably tempered martensite and ferrite microstructure. These results are in agreement with those reported by other authors [40,52].

A comparison between all surface samples is presented in Figs. 7 and 8. It can be seen that the microstructure is similar to that of the base material on the surface. Particles and slats typical of this type of steel according to literature, [40], are observable in Figs. 7 and 8. While all the samples would have to have a similar microstructure, this study could not reach a conclusion on the impact of short-time annealing.

Table 2
Characterization of samples from thermal cycle with annealing.

	A15			A9		
	Brazing temperature (°C)	Annealing temperature (°C)	Time of first cooling (s)	Brazing temperature (°C)	Annealing temperature (°C)	Time of first cooling (s)
Parameters	700	525	2	700	525	1159
Shear tests (kN)	4.32			4.22		
	A6			A5		
	Brazing temperature (°C)	Annealing temperature (°C)	Time of first cooling (s)	Brazing temperature (°C)	Annealing temperature (°C)	Time of first cooling (s)
Parameters	700	525	2	680	450	1,5
Shear tests (kN)	3.12			3.09		

Table 3
Characterization of the samples from the thermal cycle without annealing.

	S12	S9
	Brazing temperature (°C)	Brazing temperature (°C)
Parameters	720	720
Shear tests (kN)	4.59	3.94
	S4	S2
	Brazing temperature (°C)	Brazing temperature (°C)
Parameters	720	686
Shear tests (kN)	4.81	3.88

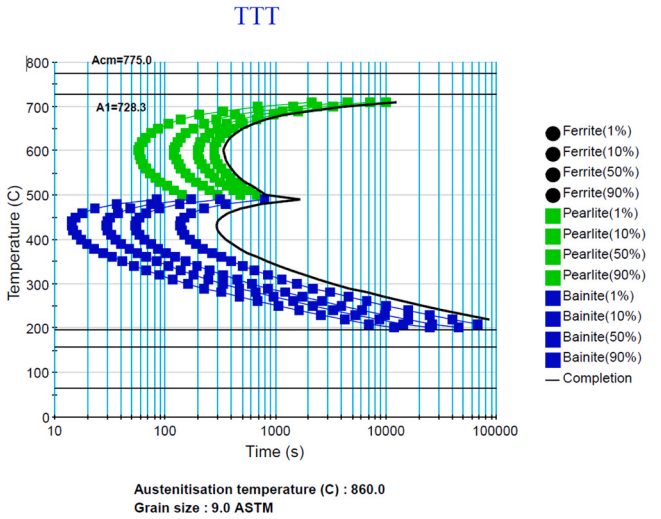

Fig. 6. TTT diagram for AISI 8670.

Further SEM analysis showed that the microstructure of the annealed samples in Fig. 7 consisted of a martensitic matrix and ferrite regions where the brazing took place close to the critical temperature (A1), as shown in TTT diagram, presented in Fig. 6. Also, some regions of tempered martensite (darker areas) were observed that contain cementite particles. By contrast, in the sample without annealing, shown in Fig. 8, the microstructure is only formed of martensite and ferrite.

It must be noted that, the hardness values presented in Fig. 10, were at the same level. This indicates that the annealing time was too short to make an impact on hardness.

3.3. Hardness

Hardness is a mechanical property that allows to distinguish one product from the other. Appropriate thermal cycle leads to the required hardness value in each zones of interest [40]. In this way, choosing the good annealing time allows to obtain the desired hardness. In this context, a CCT diagram of the AISI 8670 was created with JMATPro. Fig. 9 illustrates that with a change of time, and thus of the thermal cycle, changes can occur in terms of hardness, and can be positive or negative, depending on the desired result.

Hardness tests were conducted to observe hardness values in areas of interest and assess the impact of thermal cycle on mechanical properties. Hardness profiles were conducted on the different samples to note any changes in this mechanical property, and are presented in Fig. 10. It shows the different profiles in a single graph. It must be noted that, all the hardness profiles illustrated in Fig. 11 have been conducted in the HAZ of the steel.

In the surface direction, there are two hardness trends, in the HAZ and at the end of the HAZ. Indeed, it can be said that the HAZ affects the hardness of the samples in that it reduces the average hardness because an increase of the heating time in the zone reduces the average hardness, as shown in the CCT diagram in Fig. 9. This impact is illustrated by the difference between the profile for the base material and the other profiles in this zone. An average of 80 HV_{10} is measured between the base material profile and the others in the HAZ.

Moreover, it is important to note that some variations in hardness can be observed within the HAZ, clearly demonstrating the heterogeneous nature of the Has region. The results reported in Fig. 12 further demonstrates that it cannot be stated that a given thermal cycle has a greater impact over hardness changes than the other. For instance, S2 and A15 samples, which have received different thermal cycles, have the same hardness profile. Therefore, it can thus not be claimed that the annealing influences the hardness at the surface.

These were, however, not the only profiles studied. An analysis of the profiles in the thickness direction is required to observe the impact of the thermal cycles deep in the samples. Fig. 12 illustrates the variations of hardness in this area. The profiles follow the same trend and have the same average value of 430 $HV_{0.2}$. This can be interpreted as that even in the depths of the saw's teeth, the hardness is the same, and that the annealing that is realized has no effect on the hardness.

It can be said that in terms of hardness, there is no noticeable difference between the thermal cycles with or without short-time annealing. However, anneal is mainly used to reduce residual stress induced by thermal cycles [53]. Therefore, residual stress must be analyzed to conclude on the interest of a thermal cycle with fast annealing in an industrial context.

3.4. Residual stress

Residual stress measurements were performed at various locations on the different samples. Because the brazing process involves heating, a HAZ appeared, as illustrated in Figs. 2 and 11. This heating creates different lines on the sample all over the HAZ. In that context, the choice was made to measure the residual stress on these lines using a Pulstec device. Fig. 13 (a) shows a sample produced with heating lines.

Measurements on the surface are located in the HAZ and especially on the heating lines as illustrated in Fig. 13 (b). 3 lines of measurements

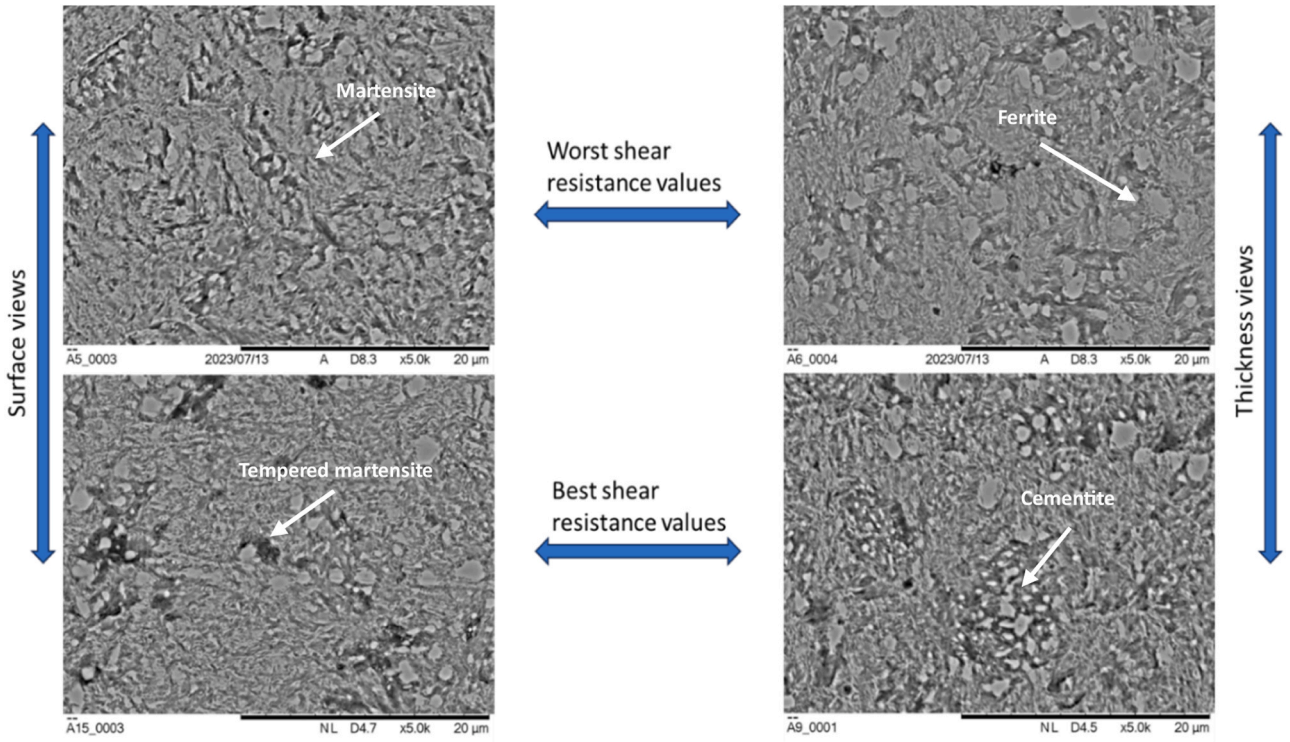

Fig. 7. - Samples views – Thermal cycle with anneal x1500.

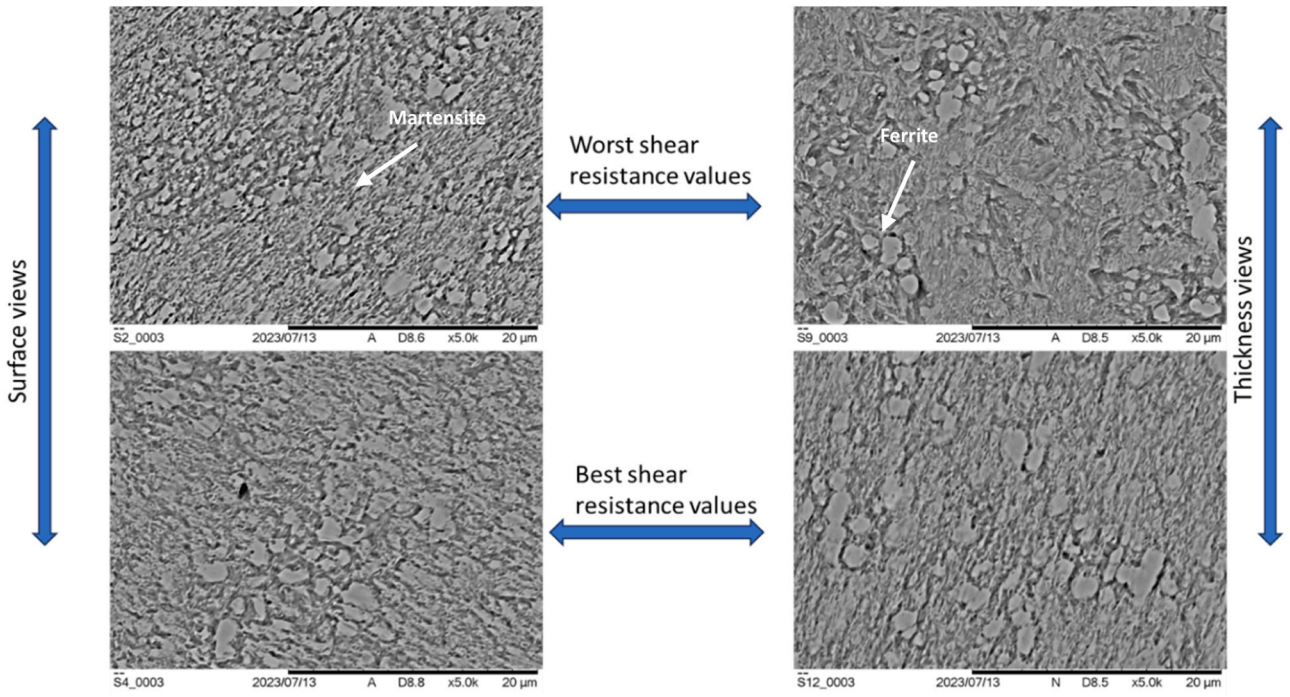

Fig. 8. - Samples views – Thermal cycle without annealing x1500.

have been conducted, referenced as lines 0, 1 and 2. Each line is composed of 3 dots, left (L), middle (M) and right (R).

Residual stress measurements were performed in the thickness direction for all the batches tested as well. 3 locations were chosen, and are illustrated as Top, Middle and Bottom in Fig. 3(b).

Measurements on the base sample were used as a reference of comparison for the other samples tested. Fig. 14 shows the residual stress measurement results for the base sample and for the other samples tested on the surface. There is no noticeable trend with respect to variations of the residual stress on the surface. However, it appears that on all the samples, the right edge contains more residual stress than the other positions. With regard to Fig. 14, it seems that as we gets closer to the edge of the sample and the brazed zone, the residual stress values measured increase. This can be explained by the fact that because of the different natures of the materials, residual stress can be produced during brazing because the materials undergo thermal expansion [17,54].

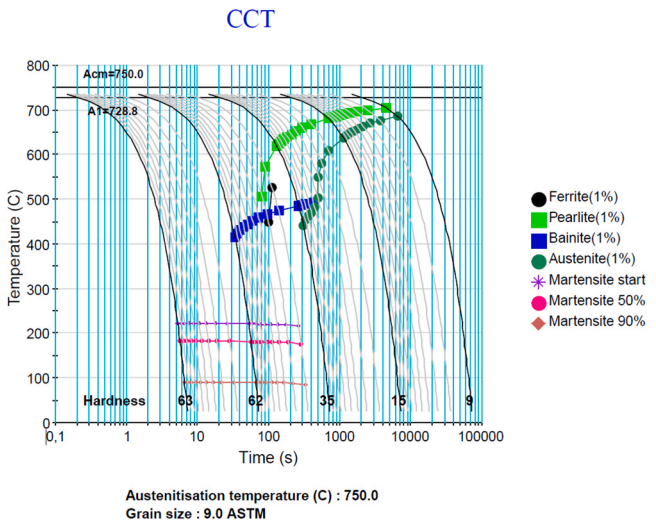

Fig. 9. - CCT diagram of AISI 8670 on JMATPro.

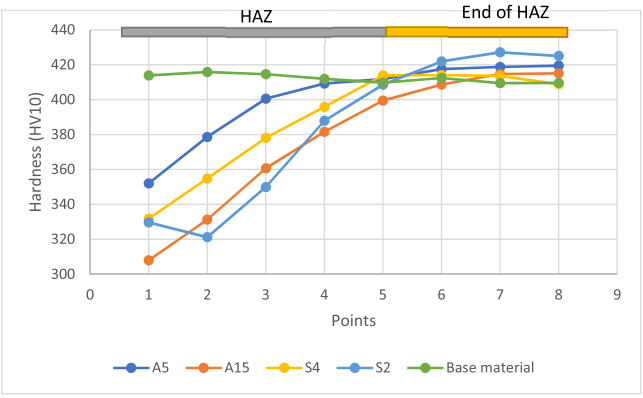

Fig. 10. - Hardness profiles in surface direction.

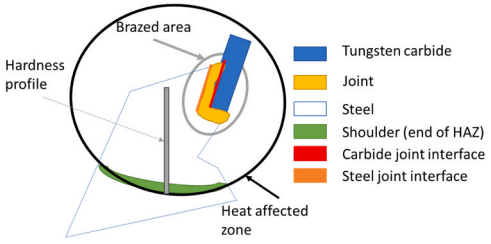

Fig. 11. - Schema of sample tested on surface with location of hardness profile.

Moreover, machining of the edges also produces stress because of the cutting forces [55,56]. In that context, more stress should naturally be present in this area. However, no noticeable changes are seen between samples having a thermal cycle with annealing and those without. Therefore, the impact of short-time annealing is not apparent. Of note though, this is not the only location where residual stress measurements can be performed. Indeed, the thickness direction is also important.

These measurements provide a better understanding of the evolution of residual stress in the samples. Indeed, it should be noted that all the samples tested have the same order of magnitude because the residual stress levels measured are all in compression, as shown in the graph in Fig. 15, regardless of the location. The values are within the − 400 to − 200 MPa interval. Negative values imply compressive residual stresses, which is interesting from an industrial point of view [57,58].

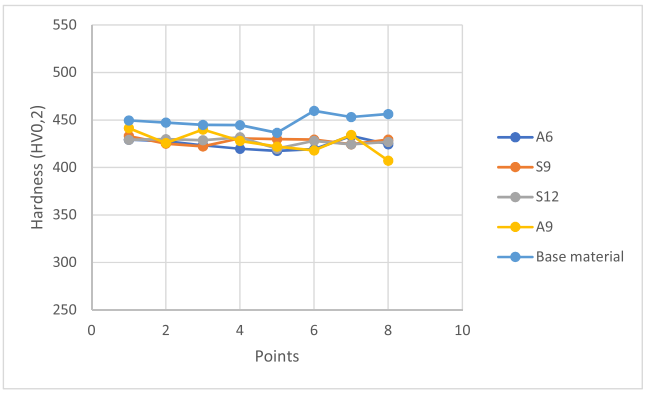

Fig. 12. - Hardness profiles in thickness direction – End of HAZ.

The main goal of the present project was to observe the impact of short-time annealing during an industrial brazing process. However, there is no noticeable difference in terms of residual stress between thermal cycles with and without annealing. For some directions, with short time annealing samples, like A6 and A9 samples, have lower residual stress in the bottom direction. But this is contrasted by other trends where without short-time annealing some samples, like S12 and S 9, have lower residual stress in middle location, as illustrated in Fig. 15. In that extent, a definitive conclusion cannot be drawn on the real impact of short-time annealing during an industrial brazing process. These results do not show any significant change in terms of residual stress in the areas of interest between samples with and without short-time annealing. The process allows to maintain compressive residual stresses in the thickness of the samples, irrespective of whether or not there is short-time annealing, as shown in Fig. 15. Yang et al. [34] show that the short-time annealing temperature influences the residual stress. However, in the present study, the short-time annealing duration was 1 s long, whereas for the Yang et al. study, it was 1 min. Moreover, Yang et al. [34] showed that there is a mutually exclusive tendency when it comes to variation of hardness and residual stress and that both cannot be improved simultaneously. The difference in time between the present study and Yang et al. study can explain the minor changes in terms of residuals stress, strength, hardness and microstructure with or without short-time annealing. To that extend, the short-time annealing as realized presently doesn't seem to have a proper impact during the production even though this is a costly and time-consuming step during the process.

4. Conclusions

The microstructure, hardness and residual stress of AISI 8670 during two different thermal cycles were investigated in this study. The following conclusions were drawn:

1. Significant correlation was not found between the IMCs layer thickness and the joint shear strength. This is probably due to the limited extent of the study on this aspect and work needs to be done to fully quantify the impact of IMC characteristics on shear strength of the joint.
2. Short-time annealing as realized in an industrial context does not seem to have a significant impact on the microstructure, hardness and residual stress.
3. The short-annealing duration seems to be too short to have a significant impact on these properties.

Declaration of Competing Interest

The authors declare that they have no known competing financial interests or personal relationships that could have appeared to influence

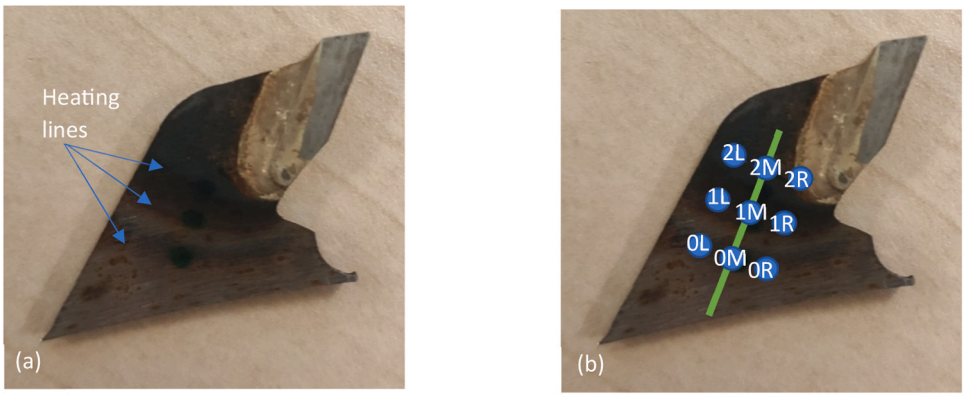

Fig. 13. - Brazed samples: (a) Illustration of the heating lines, (b) locations of measured points on Pulstec.

Fig. 14. - Residual Stress measurements on surface.

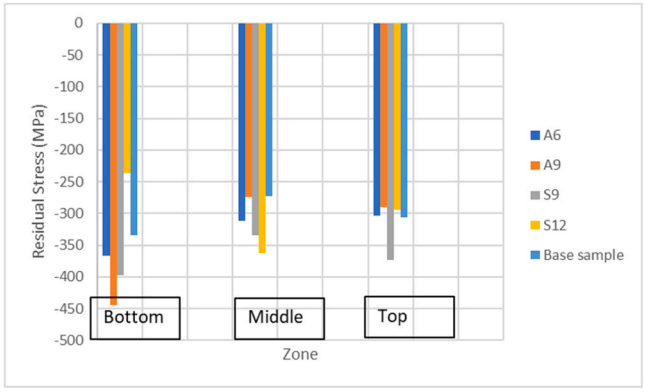

Fig. 15. - Residual stress measurements in thickness direction.

the work reported in this paper.

Acknowledgements

The authors acknowledge Consortium de recherche et d'innovation en transformation métallique (CRTIM), DK-SPEC, Natural Sciences and Engineering Research Council of Canada (NSERC), and École de Technologie Supérieure, for providing technical data, casting facilities and materials, as well as financial support. The authors thank Mr. Éric Lehoux, Mr. Hamza Sofiane Meddas, Mr. Radu Romanica, Mr. Mohammad Saadati and Mr. Mahshad Javidikia for their help during production of the samples and trainings.

References

[1] Canada, The State of Canada's Forests - Annual Report 2020, (2020) 96.
[2] S. Kashyap, T. Banik, T. Sahachar Reddy, Comparative study and modelling of machinability characteristics of single and double tempered AISI H13 steel during hard part finish turning using brazed tungsten carbide tip, Mater. Today.: Proc. 26 (2020) 1430–1438, https://doi.org/10.1016/j.matpr.2020.02.296.
[3] J. Guo, Z.Z. Fang, P. Fan, X. Wang, Kinetics of the formation of metal binder gradient in WC–Co by carbon diffusion induced liquid migration, Acta Mater. 59 (2011) 4719–4731, https://doi.org/10.1016/j.actamat.2011.04.019.
[4] Z. Wu, J. Deng, Y. Xing, H. Cheng, J. Zhao, Effect of surface texturing on friction properties of WC/Co cemented carbide, Mater. Des. 41 (2012) 142–149, https://doi.org/10.1016/j.matdes.2012.05.012.
[5] P.Q. Xu, Dissimilar welding of WC–Co cemented carbide to Ni42Fe50.9C0.6Mn3.5Nb3 invar alloy by laser–tungsten inert gas hybrid welding, Mater. Des. 32 (2011) 229–237, https://doi.org/10.1016/j.matdes.2010.06.006.
[6] H.-O. Andrén, Microstructures of cemented carbides, Mater. Des. 22 (2001) 491–498, https://doi.org/10.1016/S0261-3069(01)00006-1.
[7] W.-B. Lee, B.-D. Kwon, S.-B. Jung, Effect of bonding time on joint properties of vacuum brazed WC – Co hard metal/carbon steel using stacked Cu and Ni alloy as insert metal, Mater. Sci. Technol. 20 (2004) 1474–1478, https://doi.org/10.1179/026708304×4312.
[8] H. Chen, K. Feng, S. Wei, J. Xiong, Z. Guo, H. Wang, Microstructure and properties of WC–Co/3Cr13 joints brazed using Ni electroplated interlayer, Int. J. Refract. Met. Hard Mater. 33 (2012) 70–74, https://doi.org/10.1016/j.ijrmhm.2012.02.018.
[9] X.Z. Zhang, G.W. Liu, J.N. Tao, H.C. Shao, H. Fu, T.Z. Pan, G.J. Qiao, Vacuum Brazing of WC-8Co Cemented Carbides to Carbon Steel Using Pure Cu and Ag-28Cu as Filler Metal, J. Mater. Eng. Perform. 26 (2017) 488–494, https://doi.org/10.1007/s11665-016-2424-6.
[10] M. Paidar, K.S. Ashraff Ali, O.O. Ojo, V. Mohanavel, J. Vairamuthu, M. Ravichandran, Diffusion brazing of Inconel 617 and 321 stainless steel by using AMS 4772 Ag interlayer, J. Manuf. Process. 61 (2021) 383–395, https://doi.org/10.1016/j.jmapro.2020.11.013.
[11] A. Uysal, E. Eryildiz, E. Altan, Turning performance of bonded cutting tools with nanographene or multi-walled carbon nanotube particle-reinforced epoxy-based nanocomposite adhesives, Arab J. Sci. Eng. 44 (2019) 7737–7752, https://doi.org/10.1007/s13369-019-03876-w.
[12] M.M. Schwartz, Fundamentals of Brazing, in: D.L. Olson, T.A. Siewert, S. Liu, G. R. Edwards (Eds.), Welding, Brazing, and Soldering, ASM International, 1993, pp. 114–125, https://doi.org/10.31399/asm.hb.v06.a0001345.
[13] M.M. Schwartz, Introduction to Brazing and Soldering, in: D.L. Olson, T.A. Siewert, S. Liu, G.R. Edwards (Eds.), Welding, Brazing, and Soldering, ASM International, 1993, pp. 109–113, https://doi.org/10.31399/asm.hb.v06.a0001344.
[14] G.W. Liu, F. Valenza, M.L. Muolo, A. Passerone, SiC/SiC and SiC/Kovar joining by Ni–Si and Mo interlayers, J. Mater. Sci. 45 (2010) 4299–4307, https://doi.org/10.1007/s10853-010-4337-3.
[15] G.W. Liu, G.J. Qiao, H.J. Wang, J.F. Yang, T.J. Lu, Pressureless brazing of zirconia to stainless steel with Ag–Cu filler metal and TiH2 powder, J. Eur. Ceram. Soc. 28 (2008) 2701–2708, https://doi.org/10.1016/j.jeurceramsoc.2008.04.008.
[16] J. Felba, K.P. Friedel, P. Krull, I.L. Pobol, H. Wohlfahrt, Electron beam activated brazing of cubic boron nitride to tungsten carbide cutting tools, Vacuum 62 (2001) 171–180, https://doi.org/10.1016/S0042-207X(01)00121-X.
[17] T. Grunder, A. Piquerez, M. Bach, P. Mille, Residual stress in brazing of submicron Al2O3 to WC-Co, J. Mater. Eng. Perform. 25 (2016) 2914–2921, https://doi.org/10.1007/s11665-016-2155-8.
[18] Y. Qin, J. Feng, Active brazing carbon/carbon composite to TC4 with Cu and Mo composite interlayers, Mater. Sci. Eng.: A 525 (2009) 181–185, https://doi.org/10.1016/j.msea.2009.06.049.
[19] X.-G. Wang, X.-G. Li, C.-G. Wang, Influence of diffusion brazing parameters on microstructure and properties of Cu/Al joints, J. Manuf. Process. 35 (2018) 343–350, https://doi.org/10.1016/j.jmapro.2018.08.020.

[20] T. Torvund, Ø. Grong, O.M. Akselsen, J.H. Ulvensøen, A process model for active brazing of ceramics: Part I Growth of reaction layers, J. Mater. Sci. 31 (1996) 6215–6222, https://doi.org/10.1007/BF00354441.
[21] Janusz Kowalewski, Janusz Szczurek, Issues in vacuum brazing, (2017). ⟨https://www.secowarwick.com/wp-content/uploads/2017/03/Issues-in-vacuum-brazing-VAC.pdf⟩ (accessed February 25, 2022).
[22] S. Simões, Diffusion bonding and brazing of advanced materials, Metals 8 (2018) 959, https://doi.org/10.3390/met8110959.
[23] V.I. Lukin, V.S. Rylnikov, A.N. Afanasyev-Khodykin, A nickel-based brazing alloy for brazing creep-resisting alloys and steels, Weld. Int. 29 (2015) 567–572, https://doi.org/10.1080/09507116.2014.952498.
[24] S. Gambaro, F. Valenza, A. Passerone, G. Cacciamani, M.L. Muolo, Brazing transparent YAG to Ti6Al4V: reactivity and characterization, J. Eur. Ceram. Soc. 36 (2016) 4185–4196, https://doi.org/10.1016/j.jeurceramsoc.2016.05.022.
[25] Q. Cai, W. Liu, Y. Ma, Z. Wang, Diffusion brazing of tungsten and steel using Ti–Ni liquid phase forming interlayer, Fusion Eng. Des. 91 (2015) 67–72, https://doi.org/10.1016/j.fusengdes.2014.12.029.
[26] Y. Mao, S. Wang, L. Peng, Q. Deng, P. Zhao, B. Guo, Y. Zhang, Brazing of graphite to Cu with Cu50TiH2 + C composite filler, J. Mater. Sci. 51 (2016) 1671–1679, https://doi.org/10.1007/s10853-015-9415-0.
[27] M. Way, J. Willingham, R. Goodall, Brazing filler metals, Int. Mater. Rev. 65 (2020) 257–285, https://doi.org/10.1080/09506608.2019.1613311.
[28] Y. Sechi, T. Tsumura, K. Nakata, Dissimilar laser brazing of boron nitride and tungsten carbide, Mater. Des. 31 (2010) 2071–2077, https://doi.org/10.1016/j.matdes.2009.10.009.
[29] Y. Li, Z. Zhu, Y. He, H. Chen, C. Jiang, D. Han, J. Li, WC particulate reinforced joint by ultrasonic-associated brazing of WC-Co/35CrMo, J. Mater. Process. Technol. 238 (2016) 15–21, https://doi.org/10.1016/j.jmatprotec.2016.06.037.
[30] X.C. Liu, Y.F. Sun, T. Nagira, K. Ushioda, H. Fujii, Microstructure evolution of Cu–30Zn during friction stir welding, J. Mater. Sci. 53 (2018) 10423–10441, https://doi.org/10.1007/s10853-018-2313-5.
[31] K. Wojsyk, G. Golański, J. Jasak, J. Słania, A. Zieliński, P. Urbańczyk, Influence of the Annealing Time After Welding on the Mechanical Properties of Welded Joint of T91 Steel, Arch. Metall. Mater. 61 (2016) 1425–1430, https://doi.org/10.1515/amm-2016-0233.
[32] X. Zhang, T.-Y. Zhang, M. Wong, Y. Zohar, Residual-stress relaxation in polysilicon thin films by high-temperature rapid thermal annealing, Sens. Actuators A: Phys. 64 (1998) 109–115, https://doi.org/10.1016/S0924-4247(97)01661-0.
[33] T.O. Sedgwick, Short time annealing, J. Electrochem. Soc. 130 (1983) 484–493, https://doi.org/10.1149/1.2119736.
[34] J. Yang, K. Bu, Y. Zhou, K. Song, Y. Song, T. Huang, X. Peng, H. Liu, Y. Du, Influence of short-time annealing on the evolution of the microstructure, mechanical properties and residual stress of the C19400 alloy strips, J. Alloy. Compd. 941 (2023) 168705, https://doi.org/10.1016/j.jallcom.2023.168705.
[35] E.V. Bobruk, X. Sauvage, A.M. Zakirov, N.A. Enikeev, Tuning the structure and the mechanical properties of ultrafine grain Al–Zn alloys by short time annealing, Rev. Adv. Mater. Sci. 55 (2018) 61–68, https://doi.org/10.1515/rams-2018-0028.
[36] J. De Prado, M. Sánchez, A. Ruiz, A. Ureña, Effect of brazing temperature, filler thickness and post brazing heat treatment on the microstructure and mechanical properties of W-Eurofer joints brazed with Cu interlayers, J. Nucl. Mater. 533 (2020) 152117, https://doi.org/10.1016/j.jnucmat.2020.152117.
[37] C.N. Niu, X.G. Song, S.P. Hu, G.Z. Lu, Z.B. Chen, G.D. Wang, Effects of brazing temperature and post weld heat treatment on 7075 alloy brazed joints, J. Mater. Process. Technol. 266 (2019) 363–372, https://doi.org/10.1016/j.jmatprotec.2018.11.023.
[38] J. Gu, M. Song, S. Ni, S. Guo, Y. He, Effects of annealing on the hardness and elastic modulus of a Cu36Zr48Al8Ag8 bulk metallic glass, Mater. Des. 47 (2013) 706–710, https://doi.org/10.1016/j.matdes.2012.12.071.
[39] W.-Y. Li, C.-J. Li, H. Liao, Effect of annealing treatment on the microstructure and properties of cold-sprayed Cu coating, J. Therm. Spray. Technol. 15 (2006) 206–211, https://doi.org/10.1361/105996306×108066.
[40] H. M. Shirazi, R. Georges, R. Hernandez, C. Blais, Effect of the cross-rolling and austempering heat treatment on the microstructure, texture, and mechanical properties of a low alloyed steel used in rotary cutting tools, Int J. Adv. Manuf. Technol. 120 (2022) 3787–3804, https://doi.org/10.1007/s00170-022-08911-z.
[41] N. Saunders, U.K.Z. Guo, X. Li, A.P. Miodownik, J.-Ph Schillé, Using JMatPro to model materials properties and behavior, JOM 55 (2003) 60–65, https://doi.org/10.1007/s11837-003-0013-2.
[42] Gerling Automation, GLL Automatic precision Brazing Machine, (2023).
[43] J. Zolgharnein, A. Shahmoradi, J.B. Ghasemi, Comparative study of Box-Behnken, central composite, and Doehlert matrix for multivariate optimization of Pb (II) adsorption onto *Robinia* tree leaves: multivariate optimization, J. Chemom. 27 (2013) 12–20, https://doi.org/10.1002/cem.2487.
[44] C.L. Ngan, M. Basri, F.F. Lye, H.R. Fard Masoumi, M. Tripathy, R. Abedi Karjiban, E. Abdul-Malek, Comparison of Box–Behnken and central composite designs in optimization of fullerene loaded palm-based nano-emulsions for cosmeceutical application, Ind. Crops Prod. 59 (2014) 309–317, https://doi.org/10.1016/j.indcrop.2014.05.042.
[45] Saxonia, BrzeTec h285 Paste, (2023).
[46] Saxonia, BrazeTec 4900A, (2023).
[47] Gerling Automation, GLFPE Brazing Bond Strength measuring unit, (2023).
[48] J. Zhang, J. Xu, J. Huang, R. Liu, Y. Xiao, G. Luo, Q. Shen, High shear strength Kovar/AlN joints brazed with AgCuTi/Cu/AgCuTi sandwich composite filler, Mater. Sci. Eng.: A 862 (2023) 144435, https://doi.org/10.1016/j.msea.2022.144435.
[49] N. Yamamoto, J. Liao, S. Watanabe, K. Nakata, Effect of intermetallic compound layer on tensile strength of dissimilar friction-stir weld of a high strength Mg alloy and Al alloy, Mater. Trans. 50 (2009) 2833–2838, https://doi.org/10.2320/matertrans.M2009289.
[50] L. Li, X. Li, K. Hu, S. Qu, C. Yang, Z. Li, Effects of brazing temperature and testing temperature on the microstructure and shear strength of γ-TiAl joints, Mater. Sci. Eng.: A 634 (2015) 91–98, https://doi.org/10.1016/j.msea.2015.03.039.
[51] M.A. Mofid, E. Loryaei, Effect of bonding temperature on microstructure and intermetallic compound formation of diffusion bonded magnesium/aluminum joints, Mater. Werkst. 51 (2020) 413–421, https://doi.org/10.1002/mawe.201900080.
[52] H. M. Shirazi, R. Georges, B. Ugulino, R. Hernández, C. Blais, Application of cross-rolling and austempering–tempering to the production of rotary cutting tools, J. Mater. Sci. 57 (2022) 15612–15635, https://doi.org/10.1007/s10853-022-07597-8.
[53] O. Vöhringer, Relaxation of residual stresses by annealing or mechanical treatment. in: Residual Stresses, Elsevier,, 1987, pp. 367–396, https://doi.org/10.1016/B978-0-08-034062-3.50027-6.
[54] Z. Zhong, Z. Zhou, C. Ge, Brazing of doped graphite to Cu using stress relief interlayers, J. Mater. Process. Technol. 209 (2009) 2662–2670, https://doi.org/10.1016/j.jmatprotec.2008.06.021.
[55] N. Masmiati, A.A.D. Sarhan, M.A.N. Hassan, M. Hamdi, Optimization of cutting conditions for minimum residual stress, cutting force and surface roughness in end milling of S50C medium carbon steel, Measurement 86 (2016) 253–265, https://doi.org/10.1016/j.measurement.2016.02.049.
[56] Y.S. Liao, H.M. Lin, Mechanism of minimum quantity lubrication in high-speed milling of hardened steel, Int. J. Mach. Tools Manuf. 47 (2007) 1660–1666, https://doi.org/10.1016/j.ijmachtools.2007.01.007.
[57] H. Sasahara, The effect on fatigue life of residual stress and surface hardness resulting from different cutting conditions of 0.45%C steel, Int. J. Mach. Tools Manuf. 45 (2005) 131–136, https://doi.org/10.1016/j.ijmachtools.2004.08.002.
[58] M.N. James, Residual stress influences on structural reliability, Eng. Fail. Anal. 18 (2011) 1909–1920, https://doi.org/10.1016/j.engfailanal.2011.06.005.